Tropical Origins of the Record-breaking 2020 Summer Rainfall Extremes in East Asia

Sunyong Kim
Yonsei University
Jae-Heung Park
Pohang University of Science and Technology (POSTECH)
Jong-Seong Kug (jskug1@gmail.com)
Pohang University of Science and Technology (POSTECH)

Research Article

Keywords: rainfall, Ocean, increase, anticyclonic

Posted Date: October 26th, 2021

DOI: https://doi.org/10.21203/rs.3.rs-966527/v1

Version of Record: A version of this preprint was published at Scientific Reports on March 30th, 2022. See the published version at https://doi.org/10.1038/s41598-022-09297-4.

Abstract

The East Asian countries have experienced heavy rainfalls in boreal summer 2020. Here, we investigate the dynamical processes driving the East Asian rainfall extremes during July and August. The Indian Ocean basin warming in June can be responsible for the anticyclonic anomalies in the western North Pacific (WNP), which contribute to the zonally-elongated rainfalls in East Asia during July through an atmospheric Rossby wave train. In August, the East Asian rainfall increase is also related to the anticyclonic anomalies in the subtropical WNP, although it is located further north. It is suggested that the north tropical Atlantic warming in June partly contributes to the subtropical WNP rainfall decrease in August through a subtropical teleconnection. The rainfall decrease in the subtropical WNP region during August drives the local anticyclonic anomalies that cause the rainfall increase in East Asia. The tropical Indian Ocean anomalously warmed in June and the subtropical WNP rainfall decreased in August 2020, which played a role in modulating the WNP anticyclonic anomalies. Therefore, the record-breaking rainfalls in East Asia occurred during July and August 2020 can potentially be explained by the teleconnections induced by the tropical origins, such as tropical Indian Ocean warming and subtropical WNP rainfall decrease.

1. Introduction

The East Asian summer monsoon (EASM) is one of the most active monsoon systems, affecting the weather and climate in East Asia and of great socio-economic importance for densely populated regions. Up to two-thirds of the annual precipitation occurs during summer over East Asia, and more than 40% of the summer rainfall falls during the rainy season (Ding 1992; Oh et al. 1997; Gong and Ho 2003). In this season, the East Asian rainfall is often derived from tropical cyclone activity, the western North Pacific anticyclonic circulation (WNPAC), and a zonally elongated rainband referred to as Meiyu in China, Changma in Korea, and Baiu in Japan (Chen et al. 2004; Ding and Chan 2005). The understanding of the East Asian summer rainfall remains an outstanding challenge mainly because the East Asian region is influenced by complex interactions between tropical, and mid-high latitude systems (Tao and Chen 1987).

Studies on the mechanism of East Asian climate suggested that the WNPAC acts as an atmospheric bridge linking tropical forcing to East Asia (Chang et al. 2000; Wang et al. 2000; Lu 2001; Wang and Zhang 2002; Lee et al. 2006; Lee et al. 2013; Wang et al. 2013). It has been widely recognized that the WNPAC plays a key role in connecting the El Niño-Southern Oscillation (ENSO) to East Asia (Nitta 1987; Wang et al. 2000; Wang et al. 2003; Son et al. 2014; Gong et al. 2015; Kim et al. 2017; Kim and Kug 2018; Kim et al. 2018). Although the ENSO is known as a major driver for East Asian summer climate, the tropical Indian Ocean also contributes to the development and persistence of the WNPAC (Ohba and Ueda 2006; Wu et al. 2009; Xie et al. 2009; Wu and Yeh 2010; Hu et al. 2019) during post-El Niño summers. Additionally, the relationship between the Indian Ocean SST and East Asian summer variability has been reported (Guan and Yamagata 2003; Oh et al. 2005; Yuan et al. 2008; Kripalani et al. 2010; Kosaka et al. 2013; Xie et al. 2016; Kim and Kug 2021).

Xie et al. (2009) suggested that the warm Indian Ocean sea surface temperatures (SSTs) during post-El Niño summers can contribute to the interannual variability of the EASM. The tropical Indian Ocean warming causes the tropospheric heating via moist adiabatic adjustment (Su and Neelin 2003), which excites baroclinic Kelvin waves into the western Pacific inducing surface Ekman convergence on, and divergence off, the equator. The resultant suppressed convection and anticyclonic anomalies in the WNP may be associated with changes in the strength of the EASM. This process is known as the Indo-western Pacific Ocean capacitor (IPOC) mode, linking the tropical Indian Ocean and WNPAC in post-El Niño summer (Xie et al. 2009). The WNPAC further affects East Asia through an atmospheric Rossby wave train with meridional dipoles in the lower troposphere, the so-called Pacific–Japan (PJ) pattern (Nitta 1987).

During the summer of 2020, particularly heavy rainfall triggered flooding and landslides in the East Asian regions. Recently, it is suggested that the warm Indian Ocean condition like the super Indian Ocean Dipole (IOD) in 2019 could be related to the enhanced rainfall in East Asia during early summer 2020 (Takaya et al. 2020; Zhou et al. 2021). Liu et al. (2020) reported that the subseasonal phase transition of the North Atlantic Oscillation (NAO) played a key regulator of sequential warm/cold rainband around the Yangtze River in early summer 2020. In July 2020, the zonally elongated rainband was prominent in East Asia (Fig. 1a) striking the record-breaking rainfall event (3.07mm/day; Fig. 1b). In August 2020, relatively widespread rainfall in East Asia, including eastern Mongolia, northeastern China, and Korea, slightly migrated northward (Fig. 1c) compared to the pattern of July. The rainfall rate in August 2020 was also the largest magnitude since 1979, reaching 1.89mm/day (Fig. 1d).

In this study, the summer rainfall in East Asia, particularly during July and August, is investigated with a focus on its large-scale dynamics. Two possible key factors are suggested here: 1) tropical Indian Ocean SST during June, and 2) rainfall variability in the subtropical WNP during August. We then analyze how the tropical Indian Ocean SST and subtropical WNP rainfall affect the summer rainfall in the East Asian region. Based on the comprehensive understanding of the summer rainfall variability in East Asia, the East Asian rainfall extremes in summer 2020 will be addressed.

2. Data

The monthly precipitation data obtained from the Climate Prediction Center Merged Analysis of Precipitation (CMAP; Xie and Arkin (1997)) were used. The monthly geopotential height and horizontal wind data were from the National Center for Environmental Prediction-National Energy Research Supercomputing Center of the Department of Energy Reanalysis II (NCEP-DOE R2; Kanamitsu et al. (2002)). Both datasets have a 2.5° latitude-longitude resolution. The monthly SST data used were from the National Ocean Atmospheric Administration (NOAA) Extended Reconstructed Sea Surface Temperature version 5 (ERSSTv5; Huang et al. (2017)) with a horizontal resolution of 2° x 2°. Only the boreal summer (June-August) considered for the period from 1979 to 2020. Note that the seasonal cycle and linear trend are removed from all data before analysis.

A Linear Baroclinic Model (LBM; Watanabe and Kimoto (2000)) is used to obtain a steady atmospheric response to a prescribed diabatic forcing in the subtropical WNP. The LBM in this study is based on primitive equations linearized about the observed monthly basic state during 1979-2020. The model variables have horizontal resolution of T21 and 20 sigma levels (T21 L20). The time integration is continued for up to 30 days to approach the steady atmospheric response to a prescribed forcing in this method.

3. Results

Unusual heavy rainfall, accompanied with severe flooding and landslides, affected millions of people over large parts of the East Asian countries in summer 2020. However, the detailed patterns of rainfall in July and August exhibit some differences. In July 2020, the observed rainfalls in East Asia around the latitude of 30°N were well above normal and the highest recorded one (Fig. 1a, b). The rainfall anomaly of July 2020 in East Asia (105°-150°E, 25°-40°N) is exceeding 3.27 standard deviation for the 42-year period. In the tropics, a zonally extended rainfall decrease occurred from the Indian subcontinent to subtropical WNP, and increased in the Indian Ocean.

A relatively weak but broad rainfall increase in East Asia is the predominant feature in August 2020, evolving further to the north (Fig. 1c) compared to that of July (Fig. 1a). Because of the northward rainband, the different East Asian regions are selected in July and August based on their maximum rainfall. The rainfall magnitude of East Asia (100°-135°E, 30°-50°N) in August 2020 is above 3.0 standard deviation during the 42 years. In comparison with July, the rainfall decrease still remained in the subtropical WNP but extended further north to around Japan in August. In contrast, the rainfall anomalies from the Indian subcontinent to the South China Sea became positives in August.

The question remains, what is responsible for the rainfall extremes in East Asia during July and August? To address this, the SST and rainfall anomalies correlated with the East Asian rainfall indices in July and August are shown in Fig. 2. Recently, Kim and Kug (2021) suggested the delayed impact of Indian Ocean warming on the East Asian surface temperature variation in summer. The Indian Ocean warming in June is responsible for significant cooling over the Korea-Japan region that peaks in July with a 1-month delay. From the lead-lag correlation with July East Asian rainfall, positive correlations are evident over most of the Indian Ocean and South China Sea in June with a maximum center in the Arabian Sea and Bay of Bengal (Fig. 2a). This implies that there is a potential role of Indian Ocean SST during June in driving the rainfall increase in East Asia during July. The correlation field of rainfall has a similar spatial pattern to that of July 2020 (Fig. 1a), appearing as west-to-east elongated rainfall decrease from the eastern Indian Ocean to subtropical central Pacific and increase in the western Indian Ocean, yet only significant around the subtropical WNP and central Pacific (Fig. 2c).

The correlations between the August East Asian rainfall index and Indian Ocean SST are weaker than that of June (Fig. 2a), but still significant in the Arabian Sea (Fig. 2b). The negative SST anomalies in the adjacent region to East Asia may be a result of the increased rainfall by reducing shortwave radiation,

rather than a cause. Interestingly, the East Asian rainfall anomalies in August are highly correlated with the negative rainfall anomalies in the subtropical WNP (Fig. 2d). In particular, the WNP rainfall decrease was evident in August 2020 (Fig. 1c), suggesting an important role in modulating the East Asian rainfall increase.

As shown in Fig. 2, the highly-correlated factors in potentially explaining the East Asian rainfall are to some extent different for July and August. Given the above results, we choose two possible factors that are responsible for the East Asian summer rainfall: the tropical Indian Ocean SST in June and subtropical WNP rainfall anomalies in August. Therefore, the question arises of how the Indian Ocean SST and WNP rainfall anomalies affect the rainfall variability in East Asia during July and August, respectively. Here, we elucidate the role of two indicators on the development of rainfall in East Asia for July and August.

The delayed impact of tropical Indian Ocean SSTs in June on the East Asian rainfall anomalies in July is investigated using regression analysis (Fig. 3). Anomalous SST warming in the Indian Ocean, centered over the Arabian Sea and eastern Bay of Bengal, are quite similar that in June, suggesting strong persistency (Fig. 3a). Note that standardized coefficient refers to the regression coefficients simply multiplied by the value of the Indian Ocean SST anomaly in June 2020. In addition, the significant negative SST anomalies are zonally confined near East Asia latitude between 30°-50°N. This regressed SST pattern in July onto 1-month leading Indian Ocean warming (Fig. 3a) is quite similar to the SST anomalies of July 2020 (Fig. 3b), and has a spatial correlation (45°E-165°W, 5°S-55°N) of 0.52.

Traditionally, the tropical Indian Ocean basin warms the season after El Niño (Weare 1979), indicating a passive response to El Niño. The relative importance of remote forcing from the Pacific to the Indian sector (i.e., tropical atmospheric bridge; Klein et al. (1999)) and internal variability of the Indian Ocean is still debated within the research community (Allan et al. 2001; Baquero-Bernal et al. 2002; Hastenrath 2002; Lau and Nath 2003; Schott et al. 2009). The Indian Ocean warming was observed in the summer of 2020 possibly in accordance with the super IOD in fall 2019 (Takaya et al. 2020; Zhou et al. 2021) and/or El Niño event in the winter of 2019/20 (Qiao et al. 2021).

The rainfall responses in July onto the Indian Ocean warming in June clearly show the zonally elongated rainband in East Asia (Fig. S1). The Indian Ocean warming enhances convective activity, particularly in the Arabian Sea, because the surface moisture convergence in that region is presumably stronger in comparison with the other Indian Ocean basins (Roxy et al. 2013). Enhanced convective heating stimulates the tropospheric Kelvin waves that propagate eastward to the western Pacific. Subsequently, the Kelvin wave-induced boundary layer divergence suppresses the local convection in the WNP, and thus low-level anticyclonic anomalies develop through the atmospheric Rossby wave response, namely the IPOC mode (Xie et al. 2009).

The resultant low-level anticyclonic anomalies in the WNP are clearly seen (Fig. 3c) as a result of the Indian Ocean warming (Wu et al. 2009; Xie et al. 2009), and are a part of the meridional wave train propagating northward, the PJ teleconnection pattern (Nitta 1987). Associated with the southwesterlies on the western side of the WNP anticyclonic circulation, large amounts of water vapor can be transported

from the tropics to East Asia. Based on the moisture budget analysis, the dynamic effect due to changes in the atmospheric circulation is dominant in July (not shown). Therefore, the Indian Ocean warming in June may be responsible for the positive rainfall anomalies in East Asia in July, exhibiting a 1-month leading role. Note that the Indian Ocean warming was also observed in July 2020 (Fig. 3b), indicating a persistent SST which continuously plays a role in decreasing the WNP rainfall. The low-level atmospheric circulation anomalies in July 2020 (Fig. 3d) resemble the regressed pattern onto the June Indian Ocean warming (Fig. 3c), and the spatial correlation coefficient with geopotential height at 850 hPa is 0.66. The temporal correlation of the Indian Ocean SST during June and the East Asian rainfall anomalies during July is also strong (0.56; Fig. 3e). Importantly, the magnitude of the Indian Ocean SST in June 2020 ranks among the top four since 1979. These results imply that the tropical Indian Ocean warming in June is one of the dominant factors leading to the rainfall extremes in East Asia during July 2020.

In August, associated with the subtropical WNP rainfall index the negative local rainfall anomalies are dominant (Fig. 4a). Concurrently, pronounced rainfall increases in East Asia due to the southwesterlies corresponding to anticyclonic anomalies (Fig. 4c). Although the amplitude of regressed rainfall anomalies in East Asia is weaker than that during August 2020 (Fig. 4b), the signal is statistically significant. Importantly, a rainfall decrease was also evident in the subtropical WNP during the August 2020 (Fig. 4b). This indicates that the subtropical WNP rainfall anomalies can play an important role in increasing rainfall in East Asia during August. The simultaneous impact of Indian Ocean SST on the East Asian rainfall in August is relatively weaker than that of Indian Ocean SST in July (0.41) with a correlation coefficient of 0.34, but possibly contributes to the East Asian region.

In response to the subtropical WNP rainfall forcing in August, the anticyclonic anomalies centered at 137.5°E, 22.5°N (Fig. 4c) can be interpreted as a Rossby wave response. The subtropical diabatic forcing in August is far from the equator, thus the wave response can be established at a relatively higher latitude. The resultant anticyclonic flow is accompanied by southwesterly anomalies from the off-equatorial towards East Asia and contributes to the rainfall anomalies there in August. Overall, the atmospheric pattern in August 2020 is quite similar to the regressed result (Fig. 4c), with anticyclonic anomalies evidently centered south of Japan (Fig. 4d). The spatial correlation coefficient between these low-level patterns represented as the geopotential heights at 850 hPa is 0.66. The distribution of subtropical WNP rainfall and East Asian rainfall anomalies for the period 1979-2020 also indicates a significant relationship with a correlation coefficient of -0.56 (Fig. 4e). In August 2020, the magnitude of the subtropical WNP rainfall anomaly ranks 4th over the last 42 years. This implies that in August the subtropical WNP rainfall decrease may contribute to the development of anticyclonic anomalies, affecting the extreme East Asian rainfall.

To examine atmospheric response to the subtropical diabatic forcing, the LBM (Watanabe and Kimoto (2000)) experiment is carried out (Fig. 5). In this experiment, the prescribed forcing is obtained from the linearly regressed local rainfall with respect to the subtropical WNP rainfall index in August (Fig. 4a), using August basic state during 1979-2020. It is evident that the negative rainfall forcing over the subtropical WNP region (Fig. 5a) is critical in developing the anticyclonic circulation (Fig. 5b), matching

well the observational pattern (Fig. 4c). Therefore, the subtropical WNP anticyclonic anomalies can be explained by the negative local rainfall anomalies through the atmospheric Rossby wave response, and then play an important role in modulating the East Asian rainfall in August.

Importantly, the rainfall extremes in July and August 2020 showed different features in East Asia, as a zonally-elongated rainband located near 30°N in July (Fig. 1a), and a relatively broad one confined further north of 30°N in August (Fig. 1c). At the same time, the dominant negative rainfall anomalies over the WNP region are also distinct in July and August, showing that it moves further northeastward in accordance with the northward shifted rainfall in East Asia during August (Fig. 2d), compared to the pattern of July (Fig. 2c). Both the WNP rainfall anomalies in July and August may play an important role in modulating the rainfall variability in East Asia, respectively, although their magnitude and location are different.

However, it is not certain whether the July WNP rainfall evolves to the August one, or another physical process induces the August rainfall independently. To understand the rainfall variability over the subtropical WNP region in August, its preceding SST and rainfall patterns are investigated (Fig. S2). The positive local SST anomalies are dominant in June then persist until July, linking to the subtropical WNP rainfall increase in August. However, in August the local SST correlations turn negatives located near 30°N, which can be regarded as a result of rainfall increase rather than a cause. Interestingly, the north tropical Atlantic (NTA) warming in June is significantly correlated with the subtropical WNP rainfall anomalies in August with 2-month leading role, but the correlations over the NTA region become weaker after June. As suggested in Ham et al. (2013), the NTA warming during the spring can induce the low-level cyclonic flow over the eastern Pacific that in turn triggers the low-level anticyclonic flow over the western Pacific in the following months through a subtropical teleconnection. Therefore, the NTA SST anomalies possibly have an impact on the East Asian summer variability through the WNP anticyclonic anomalies (Jin and Huo 2018).

The lagged regressions of SST, rainfall and wind responses at 850 hPa to the NTA (50°-15°W, 0°-20°N) SST anomalies in June are shown in Fig. 6. In June, the positive SST anomalies in the NTA region (Fig. 6a) enhances the local convective activity (Fig. 6d). The resultant diabatic heating gives rise to the low-level cyclonic anomalies over the subtropical eastern Pacific in July as a Gill-type response, with the northerly anomalies on its western side (Fig. 6e). In July, the zonally-elongated rainband in East Asia are quite similar with the observed July 2020 (Fig. 1a), suggesting the potential role of NTA SST anomalies. The northerlies in the subtropical Pacific induce the surface cooling through the enhanced wind speed and cold/dry advection from higher latitudes. As a result, the negative rainfall anomalies in the subtropical Pacific induce the subtropical WNP anticyclonic flow until August through the strong air-sea coupling (Fig. 6f). The associated rainfall decrease and anticyclonic circulation in the subtropical WNP region possibly affect the summer rainfall in East Asia during August. The NTA-regressed rainfall increase in East Asia during August is significant (Fig. 6f) and quite similar with that of August 2020 (Fig. 1c). This implies that the NTA warming in June can play a role in modulating the East Asian rainfall

in August through the development of subtropical WNP anticyclonic anomalies with 2-month time lag. In June 2020, the NTA region anomalously warmed that is above 0.92 standard deviation during 1979-2020.

Additionally, relatively stronger mean and variability of rainfall exist in the subtropical WNP region during August compared to that during July (not shown) due to the northward migration of the Pacific Intertropical Convergence Zone (ITCZ). Therefore, the interannual variability of subtropical WNP rainfall may well be sensitive to the relatively enhanced climatological local rainfall from July to August. It provides favorable conditions such that enhancement of convective instability in the subtropical WNP extends further north during August. As a result, this strengthened rainfall variability in the subtropical WNP during August may play a more dominant role in modulating local anticyclonic anomalies, and have a profound impact on the East Asian rainfall anomalies.

4. Summary And Discussion

In the 2020 summer, extraordinary rainfall extremes hit East Asia. We show that the tropical Indian Ocean SST and subtropical WNP rainfall anomalies can indeed be responsible for the East Asian rainfall anomalies during July and August, respectively. The Indian Ocean basin warming through the summer 2020, extensively considered as a result of super IOD in fall 2019 and El Niño event in preceding winter, possibly modulated the anticyclonic circulation anomalies in the WNP (Xie et al. 2009). The WNP anticyclonic anomalies induce the poleward propagating wave train pattern (Nitta 1987), then the southwesterly anomalies in between the meridional atmospheric dipoles resulted in the rainfall increase in East Asia during July 2020. In August 2020, the widespread rainfall increase in the East Asian region was potentially explained by the southwesterlies associated with the subtropical WNP anticyclonic anomalies, interpreting as a Rossby wave response to the negative local rainfall anomalies. The NTA warming in summer 2020 might be responsible for the development of subtropical WNP anticyclonic anomalies in August 2020, through a subtropical Pacific teleconnection suggested in Ham et al. (2013). Additionally, due to the northward migration of Pacific ITCZ, the interannual variability of subtropical WNP rainfall is more favorable conditions that enhanced convection extends further north in August compared that of July.

It remains an outstanding challenge to predict summer rainfall variability in East Asia, mainly because of the complex climate interaction among signals originating from both the tropics and extratropics. In this study, using reanalysis data the impacts of the tropical Indian Ocean SST and subtropical WNP rainfall forcing on the summer rainfall development in East Asia are investigated. Although the influence of tropical and subtropical originating teleconnections on the East Asian rainfall anomalies are evident here, there may exist other climate factors that contributed to the rainfall extremes in East Asia during summer 2020. In the temporal relationships of tropical forcing and East Asian rainfall anomalies, the anomaly of 2020 lies far away from the linear regression line (red dot in Fig. 3e, 4e). The tropical Indian Ocean SST in June and subtropical WNP rainfall anomalies in August can potentially explain about 31% of the rainfall variability in East Asia during July and August, respectively.

Qiao et al. (2021) suggested the relative roles of tropical and extratropical factors in different stages of the East Asian rainfall evolution in summer 2020. The development of La Niña also could be a responsible for the enhanced WNP anticyclonic flow and East Asian rainfalls (Kosaka et al. 2012; Wang et al. 2013). The relatively weak cooling in the equatorial central Pacific in August 2020 (Fig. S1) might contribute to the negative local rainfall anomalies (Fig. 1c), leading anticyclonic anomalies to its west and depressed convection over the subtropical WNP (Gill 1980). A wave train related to the NAO emerges downstream along with the polar-front jet, and then modulate the summer rainfall variability around the Yangtze River in summer 2020 (Liu et al. 2020). In addition, the rainfall increase over India (Fig. 1c) associated with the SST warming in the Arabian Sea possibly excited Rossby wave propagation towards East Asia, known as the circumglobal teleconnection (CGT) pattern (Ding and Wang 2005). Therefore, relative roles of the tropical, extratropical, and polar origins in the East Asian summer climate will be further pursued.

Under global warming scenarios, summer rainfall in the East Asian region is projected to likely increase (Kripalani et al. 2007; Lu and Fu 2010; Kusunoki and Arakawa 2012; Chen and Sun 2013; Kitoh et al. 2013). However, uncertainties in the projections of future rainfall changes in East Asia among climate models are also large (Hsu et al. 2013; Sooraj et al. 2015; Zhou et al. 2017). Therefore, understanding the future changes of two possible teleconnection pathways, from the tropical Indian Ocean and subtropical WNP regions, are of great importance for regional rainfall variability in East Asia during summer. Model experiments incorporating future climate change will also provide assessment of the future subseasonal rainfall variability in East Asia associated with the tropical Indian Ocean SST and subtropical WNP rainfall forcings.

Declarations

Data Availability Statement

The monthly rainfall data were provided by the Center for Climate Prediction Merged Analysis of Rainfall (CMAP), from their website at https://psl.noaa.gov/data/gridded/data.cmap.html. The monthly atmospheric variables by the National Center for Environmental Prediction-National Energy Research Supercomputing Center of the Department of Energy Reanalysis II (NCEP-DOE R2) were obtained from https://psl.noaa.gov/data/gridded/data.ncep.reanalysis2.html. The monthly SST data used from the National Ocean Atmospheric Administration (NOAA) Extended Reconstructed Sea Surface Temperature version 5 (ERSSTv5) were available from https://psl.noaa.gov/data/gridded/data.noaa.ersst.v5.html.

Conflict of Interest

The authors declare that they have no conflict of interest.

References

1. Allan R, Chambers D, Drosdowsky W, Hendon H, Latif M, Nicholls N, Smith I, Stone R, Tourre Y (2001) Is there an Indian Ocean dipole and is it independent of the El Niño-Southern Oscillation. CLIVAR Exchanges 6: 18–22
2. Xie, S-P. *et al.* Indian Ocean capacitor effect on Indo–western Pacific climate during the summer following El Niño. *Journal of Climate*, **22**, 730–747 https://doi.org/10.1175/2008JCLI2544.1 (2009).
3. Xie, S-P. *et al.* Indo-western Pacific ocean capacitor and coherent climate anomalies in post-ENSO summer: A review. *Advances in Atmospheric Sciences*, **33**, 411–432 https://doi.org/10.1007/s00376-015-5192-6 (2016).
4. Yuan, Y., Yang, H., Zhou, W. & Li, C. Influences of the Indian Ocean dipole on the Asian summer monsoon in the following year. *International Journal of Climatology*, **28**, 1849–1859 https://doi.org/10.1002/joc.1678 (2008).
5. Zhou, T. *et al.* A robustness analysis of CMIP5 models over the East Asia-Western North Pacific domain. *Engineering*, **3**, 773–778 https://doi.org/10.1016/J.ENG.2017.05.018 (2017).
6. Zhou, Z-Q., Xie, S-P. & Zhang, R. (2021) Historic Yangtze flooding of 2020 tied to extreme Indian Ocean conditions. Proceedings of the National Academy of Sciences 118 https://doi.org/10.1073/pnas.2022255118.
7. Ding Y (1992) Summer monsoon rainfalls in China. Journal of the Meteorological Society of Japan 70: 373-396 https://doi.org/10.2151/jmsj1965.70.1B_373.
8. Ding Y, Chan JC (2005) The East Asian summer monsoon: an overview. Meteorology Atmospheric Physics 89: 117-142 https://doi.org/10.1007/s00703-005-0125-z.
9. Gill AE (1980) Some simple solutions for heat-induced tropical circulation. Quarterly Journal of the Royal Meteorological Society 106: 447-462 https://doi.org/10.1002/qj.49710644905.
10. Gong DY, Ho CH (2003) Arctic oscillation signals in the East Asian summer monsoon. Journal of Geophysical Research: Atmospheres 108 https://doi.org/10.1029/2002JD002193.
11. Gong H, Wang L, Chen W, Nath D, Huang G, Tao W (2015) Diverse influences of ENSO on the East Asian–western Pacific winter climate tied to different ENSO properties in CMIP5 models. Journal of Climate 28: 2187-2202 https://doi.org/10.1175/JCLI-D-14-00405.1.
12. Guan Z, Yamagata T (2003) The unusual summer of 1994 in East Asia: IOD teleconnections. Geophysical Research Letters 30 https://doi.org/10.1029/2002GL016831.
13. Ham Y-G, Kug J-S, Park J-Y, Jin F-F (2013) Sea surface temperature in the north tropical Atlantic as a trigger for El Niño/Southern Oscillation events. Nature Geoscience 6: 112-116 https://doi.org/10.1038/ngeo1686.
14. Hastenrath S (2002) Dipoles, temperature gradients, and tropical climate anomalies. Bulletin of the American Meteorological Society 83: 735-738 https://doi.org/10.1175/1520-0477(2002)083<0735:WLACNM>2.3.CO;2.
15. Hsu Pc, Li T, Murakami H, Kitoh A (2013) Future change of the global monsoon revealed from 19 CMIP5 models. Journal of Geophysical Research: Atmospheres 118: 1247-1260 https://doi.org/10.1002/jgrd.50145.

16. Hu K, Huang G, Xie S-P, Long S-M (2019) Effect of the mean flow on the anomalous anticyclone over the Indo-Northwest Pacific in post-El Niño summers. Climate Dynamics 53: 5725-5741 https://doi.org/10.1007/s00382-019-04893-z.
17. Huang B, Thorne PW, Banzon VF, Boyer T, Chepurin G, Lawrimore JH, Menne MJ, Smith TM, Vose RS, Zhang H-M (2017) Extended reconstructed sea surface temperature, version 5 (ERSSTv5): upgrades, validations, and intercomparisons. Journal of Climate 30: 8179-8205 https://doi.org/10.1175/JCLI-D-16-0836.1.
18. Jin D, Huo L (2018) Influence of tropical Atlantic sea surface temperature anomalies on the East Asian summer monsoon. Quarterly Journal of the Royal Meteorological Society 144: 1490-1500 https://doi.org/10.1002/qj.3296.
19. Kanamitsu M, Ebisuzaki W, Woollen J, Yang S-K, Hnilo J, Fiorino M, Potter G (2002) NCEP–DOE AMIP-II Reanalysis (R-2). Bulletin of the American Meteorological Society 83: 1631-1644 https://doi.org/10.1175/BAMS-83-11-1631.
20. Kim S, Kug J-S (2021) Delayed impact of Indian Ocean warming on the East Asian surface temperature variation in boreal summer. Journal of Climate: 1-40 https://doi.org/10.1175/JCLI-D-20-0691.1.
21. Kim S, Kug JS (2018) What controls ENSO teleconnection to East Asia? Role of western North Pacific precipitation in ENSO teleconnection to East Asia. Journal of Geophysical Research: Atmospheres 123: 10,406-410,422 https://doi.org/10.1029/2018JD028935.
22. Kim S, Son H-Y, Kug J-S (2017) How well do climate models simulate atmospheric teleconnctions over the North Pacific and East Asia associated with ENSO? Climate Dynamics 48: 971-985 https://doi.org/10.1007/s00382-016-3121-8.
23. Kim S, Son H-Y, Kug J-S (2018) Relative roles of equatorial central Pacific and western North Pacific precipitation anomalies in ENSO teleconnection over the North Pacific. Climate Dynamics 51: 4345-4355 https://doi.org/10.1007/s00382-017-3779-6.
24. Kitoh A, Endo H, Krishna Kumar K, Cavalcanti IF, Goswami P, Zhou T (2013) Monsoons in a changing world: A regional perspective in a global context. Journal of Geophysical Research: Atmospheres 118: 3053-3065 https://doi.org/10.1002/jgrd.50258.
25. Klein SA, Soden BJ, Lau N-C (1999) Remote sea surface temperature variations during ENSO: Evidence for a tropical atmospheric bridge. Journal of Climate 12: 917-932 https://doi.org/10.1175/1520-0442(1999)012<0917:RSSTVD>2.0.CO;2.
26. Kosaka Y, Chowdary J, Xie S-P, Min Y-M, Lee J-Y (2012) Limitations of seasonal predictability for summer climate over East Asia and the northwestern Pacific. Journal of Climate 25: 7574-7589 https://doi.org/10.1175/JCLI-D-12-00009.1.
27. Kosaka Y, Xie S-P, Lau N-C, Vecchi GA (2013) Origin of seasonal predictability for summer climate over the Northwestern Pacific. Proceedings of the National Academy of Sciences 110: 7574-7579 https://doi.org/10.1073/pnas.1215582110.

28. Kripalani R, Oh J, Chaudhari H (2007) Response of the East Asian summer monsoon to doubled atmospheric CO 2: Coupled climate model simulations and projections under IPCC AR4. Theoretical Applied Climatology 87: 1-28 https://doi.org/10.1007/s00704-006-0238-4.
29. Kripalani R, Oh J, Chaudhari H (2010) Delayed influence of the Indian Ocean Dipole mode on the East Asia–West Pacific monsoon: possible mechanism. International Journal of Climatology 30: 197-209 https://doi.org/10.1002/joc.1890.
30. Kusunoki S, Arakawa O (2012) Change in the precipitation intensity of the East Asian summer monsoon projected by CMIP3 models. Climate Dynamics 38: 2055-2072 https://doi.org/10.1007/s00382-011-1234-7.
31. Lau N-C, Nath MJ (2003) Atmosphere–ocean variations in the Indo-Pacific sector during ENSO episodes. Journal of Climate 16: 3-20
32. Lee EJ, Yeh SW, Jhun JG, Moon BK (2006) Seasonal change in anomalous WNPSH associated with the strong East Asian summer monsoon. Geophysical Research Letters 33 https://doi.org/10.1029/2006GL027474.
33. Lee S-S, Seo Y-W, Ha K-J, Jhun J-G (2013) Impact of the western North Pacific subtropical high on the East Asian monsoon precipitation and the Indian Ocean precipitation in the boreal summertime. Asia-Pacific Journal of Atmospheric Sciences 49: 171-182 https://doi.org/10.1007/s13143-013-0018-x.
34. Liu B, Yan Y, Zhu C, Ma S, Li J (2020) Record-Breaking Meiyu Rainfall Around the Yangtze River in 2020 Regulated by the Subseasonal Phase Transition of the North Atlantic Oscillation. Geophysical Research Letters 47: e2020GL090342 https://doi.org/10.1029/2020GL090342.
35. Lu R (2001) Interannual variability of the summertime North Pacific subtropical high and its relation to atmospheric convection over the warm pool. Journal of the Meteorological Society of Japan 79: 771-783 https://doi.org/10.2151/jmsj.79.771.
36. Lu R, Fu Y (2010) Intensification of East Asian summer rainfall interannual variability in the twenty-first century simulated by 12 CMIP3 coupled models. Journal of Climate 23: 3316-3331 https://doi.org/10.1175/2009JCLI3130.1.
37. Nitta T (1987) Convective activities in the tropical western Pacific and their impact on the Northern Hemisphere summer circulation. Journal of the Meteorological Society of Japan 65: 373-390 https://doi.org/10.2151/jmsj1965.65.3_373.
38. Oh J-H, Chaudhari H, Kripalani R (2005) Impact of IODM and ENSO on the East Asian monsoon: Simulations through NCAR community atmospheric model. Korean Journal of Agricultural Forest Meteorology 7: 240-249
39. Oh J-H, Kwon W-T, Ryoo S-B (1997) Review of the researches on Changma and future observational study (KORMEX). Advances in Atmospheric Sciences 14: 207-222 https://doi.org/10.1007/s00376-997-0020-2.
40. Ohba M, Ueda H (2006) A role of zonal gradient of SST between the Indian Ocean and the western Pacific in localized convection around the Philippines. Sola 2: 176-179

https://doi.org/10.2151/sola.2006-045.

41. Qiao S, Chen D, Wang B, Cheung HN, Liu F, Cheng J, Tang S, Zhang Z, Feng G, Dong W (2021) The longest 2020 Meiyu season over the past 60 years: Subseasonal perspective and its predictions. Geophysical Research Letters: e2021GL093596 https://doi.org/10.1029/2021GL093596.
42. Roxy M, Tanimoto Y, Preethi B, Terray P, Krishnan R (2013) Intraseasonal SST-precipitation relationship and its spatial variability over the tropical summer monsoon region. Climate Dynamics 41: 45-61 https://doi.org/10.1007/s00382-012-1547-1.
43. Schott FA, Xie SP, McCreary Jr JP (2009) Indian Ocean circulation and climate variability. Reviews of Geophysics 47 https://doi.org/10.1029/2007RG000245.
44. Son H-Y, Park J-Y, Kug J-S, Yoo J, Kim C-H (2014) Winter precipitation variability over Korean Peninsula associated with ENSO. Climate Dynamics 42: 3171-3186 https://doi.org/10.1007/s00382-013-2008-1.
45. Sooraj K, Terray P, Mujumdar M (2015) Global warming and the weakening of the Asian summer monsoon circulation: assessments from the CMIP5 models. Climate Dynamics 45: 233-252 https://doi.org/10.1007/s00382-014-2257-7.
46. Su H, Neelin JD (2003) The scatter in tropical average precipitation anomalies. Journal of Climate 16: 3966-3977 https://doi.org/10.1175/1520-0442(2003)016<3966:TSITAP>2.0.CO;2.
47. Takaya Y, Ishikawa I, Kobayashi C, Endo H, Ose T (2020) Enhanced Meiyu-Baiu Rainfall in Early Summer 2020: Aftermath of the 2019 Super IOD Event. Geophysical Research Letters 47: e2020GL090671 https://doi.org/10.1029/2020GL090671.
48. Tao SY, Chen L (1987) A review of recent research on the East Asian summer monsoon in China. Monsoon meteorology: 60-92
49. Wang B, Wu R, Fu X (2000) Pacific–East Asian teleconnection: how does ENSO affect East Asian climate? Journal of Climate 13: 1517-1536 https://doi.org/10.1175/1520-0442(2000)013<1517:PEATHD>2.0.CO;2.
50. Wang B, Wu R, Li T (2003) Atmosphere–warm ocean interaction and its impacts on Asian–Australian monsoon variation. Journal of Climate 16: 1195-1211 https://doi.org/10.1175/1520-0442(2003)16<1195:AOIAII>2.0.CO;2.
51. Wang B, Xiang B, Lee J-Y (2013) Subtropical high predictability establishes a promising way for monsoon and tropical storm predictions. Proceedings of the National Academy of Sciences 110: 2718-2722 https://doi.org/10.1073/pnas.1214626110.
52. Wang B, Zhang Q (2002) Pacific–east Asian teleconnection. Part II: How the Philippine Sea anomalous anticyclone is established during El Nino development. Journal of Climate 15: 3252-3265 https://doi.org/10.1175/1520-0442(2002)015<3252:PEATPI>2.0.CO;2.
53. M, Kimoto M (2000) Atmosphere-ocean thermal coupling in the North Atlantic: A positive feedback. Quarterly Journal of the Royal Meteorological Society 126: 3343-3369 https://doi.org/10.1002/qj.49712657017.

54. Weare BC (1979) A statistical study of the relationships between ocean surface temperatures and the Indian monsoon. Journal of the Atmospheric Sciences 36: 2279-2291 https://doi.org/10.1175/1520-0469(1979)036<2279:ASSOTR>2.0.CO;2.
55. Wu B, Zhou T, Li T (2009) Contrast of rainfall–SST relationships in the western North Pacific between the ENSO-developing and ENSO-decaying summers. Journal of Climate 22: 4398-4405 https://doi.org/10.1175/2009JCLI2648.1.
56. Wu R, Yeh SW (2010) A further study of the tropical Indian Ocean asymmetric mode in boreal spring. Journal of Geophysical Research: Atmospheres 115 https://doi.org/10.1029/2009JD012999.
57. Xie P, Arkin PA (1997) Global precipitation: A 17-year monthly analysis based on gauge observations, satellite estimates, and numerical model outputs. Bulletin of the American Meteorological Society 78: 2539-2558 https://doi.org/10.1175/1520-0477(1997)078<2539:GPAYMA>2.0.CO;2.
58. Xie S-P, Hu K, Hafner J, Tokinaga H, Du Y, Huang G, Sampe T (2009) Indian Ocean capacitor effect on Indo–western Pacific climate during the summer following El Niño. Journal of Climate 22: 730-747 https://doi.org/10.1175/2008JCLI2544.1.
59. Xie S-P, Kosaka Y, Du Y, Hu K, Chowdary JS, Huang G (2016) Indo-western Pacific ocean capacitor and coherent climate anomalies in post-ENSO summer: A review. Advances in Atmospheric Sciences 33: 411-432 https://doi.org/10.1007/s00376-015-5192-6.
60. Yuan Y, Yang H, Zhou W, Li C (2008) Influences of the Indian Ocean dipole on the Asian summer monsoon in the following year. International Journal of Climatology 28: 1849-1859 https://doi.org/10.1002/joc.1678.
61. Zhou T, Chen X, Wu B, Guo Z, Sun Y, Zou L, Man W, Zhang L, He C (2017) A robustness analysis of CMIP5 models over the East Asia-Western North Pacific domain. Engineering 3: 773-778 https://doi.org/10.1016/J.ENG.2017.05.018.
62. Zhou Z-Q, Xie S-P, Zhang R (2021) Historic Yangtze flooding of 2020 tied to extreme Indian Ocean conditions. Proceedings of the National Academy of Sciences 118 https://doi.org/10.1073/pnas.2022255118.

Figures

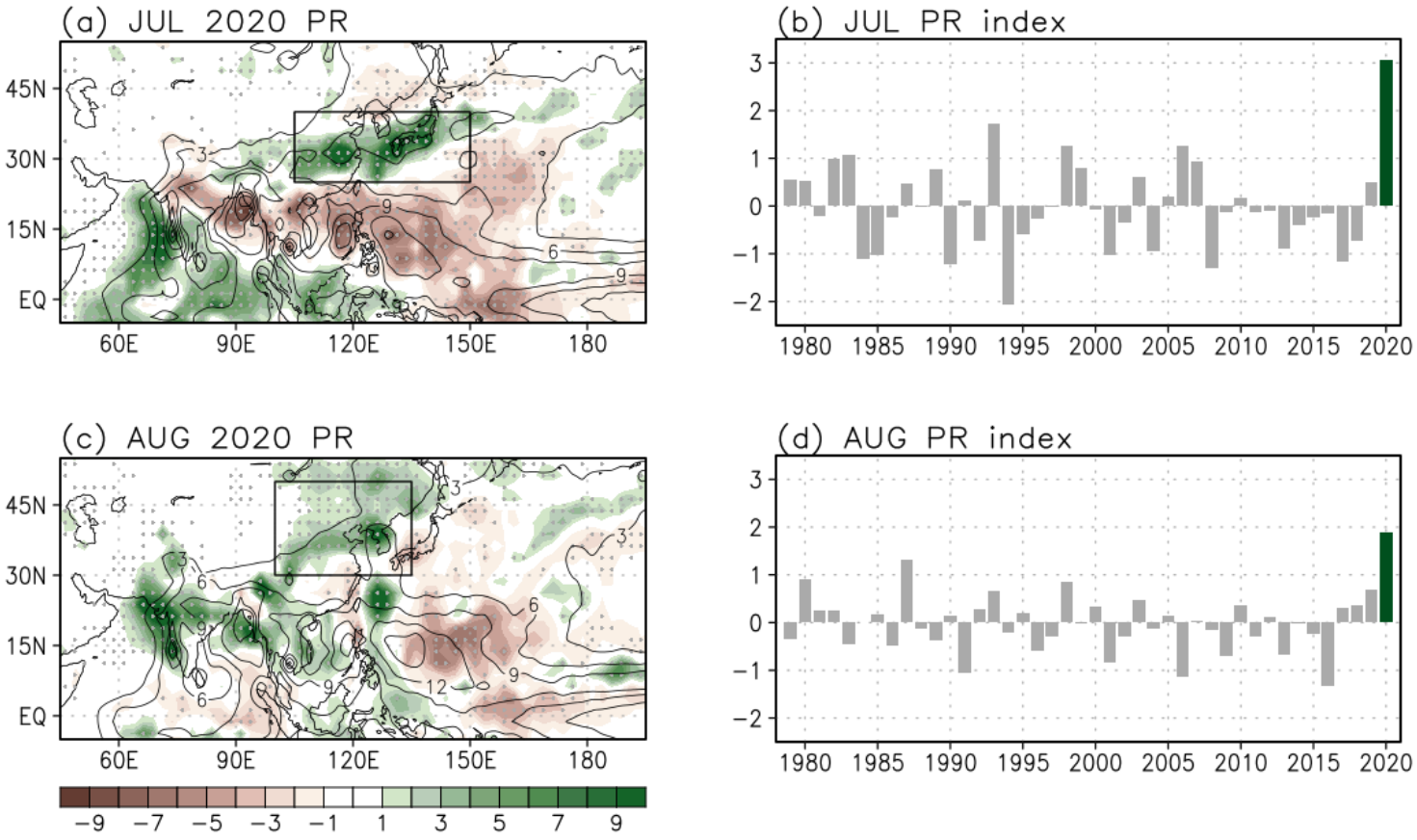

Figure 1

Rainfall climatology (contour; mm/day) in (a) July and (c) August, and anomalies (shading) in 2020. Values over the 1 standard deviation are stippled. The East Asian regions for July (105°-150°E, 25°-40°N) and August (100°-135°E, 30°-50°N) are indicated by the black-outlined rectangles. Time series of the area-averaged rainfall index in East Asia for (b) July and (d) August during 1979-2020. The rainfall values of 2020 are in green bars.

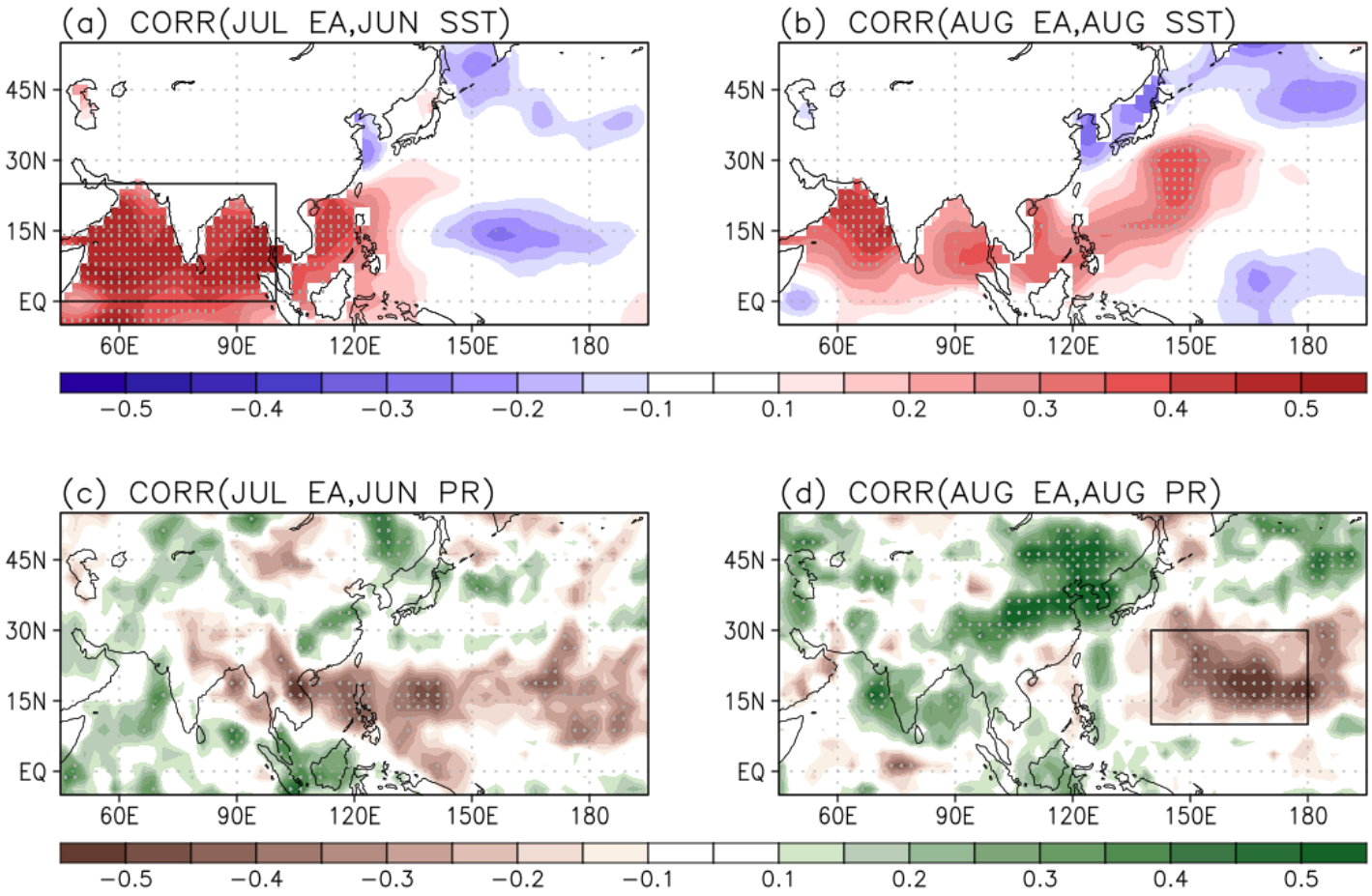

Figure 2

Correlation coefficients of the rainfall index in East Asia (105°-150°E, 25°-40°N) in July for (a) SST and (c) rainfall anomalies in June during 1979-2020. The same as in (b) and (d) but for August and the rainfall index in East Asia (100°-135°E, 30°-50°N) in August. Values over the 95% confidence level based on the student t-test are stippled. The SST anomalies in the tropical Indian Ocean (a; 45°-100°E, 0°-25°N) and rainfall anomalies in the subtropical WNP (d; 140°E-180°, 10°-30°N) region are indicated by the black-outlined rectangles.

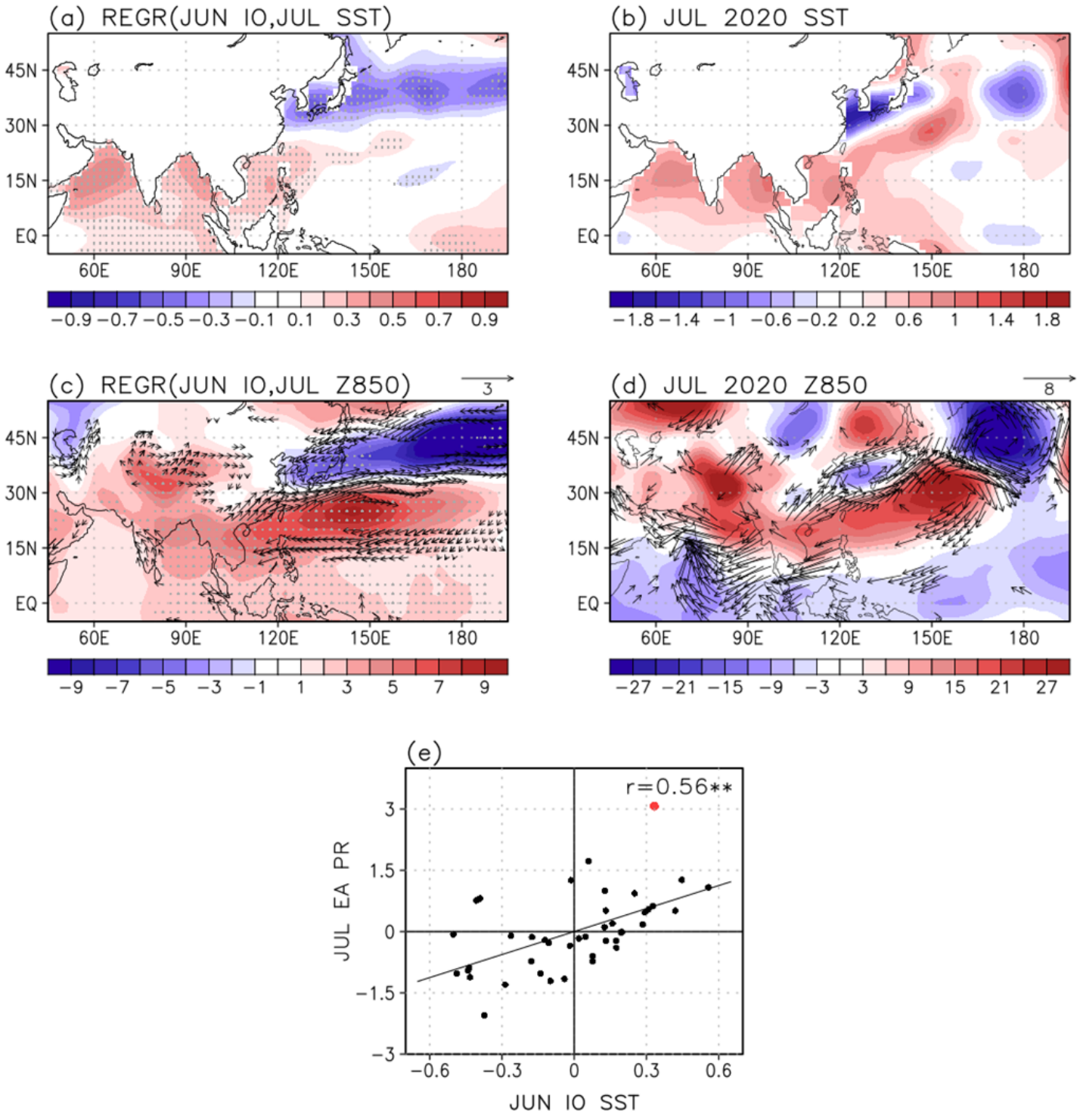

Figure 3

Regressed (a) SST (℃), (c) geopotential height (shading; m) and wind (vectors; m/s) anomalies at 850 hPa in July onto the Indian Ocean (45°-100°E, 0°-25°N) SST in June during 1979-2020. Note that the regression coefficients are multiplied by the value of Indian Ocean SST in June 2020. Values over the 95% confidence level based on the student t-test are stippled and represented as vectors. (b) SST, (d) geopotential height and wind anomalies at 850 hPa in July 2020. (e) Scatter diagram between the Indian

Ocean SST in June and East Asian (105°-150°E, 25°-40°N) rainfall index in July. The value for 2020 is indicated by the red dot. The symbol of ** denotes the 99% confidence level based on the student t-test.

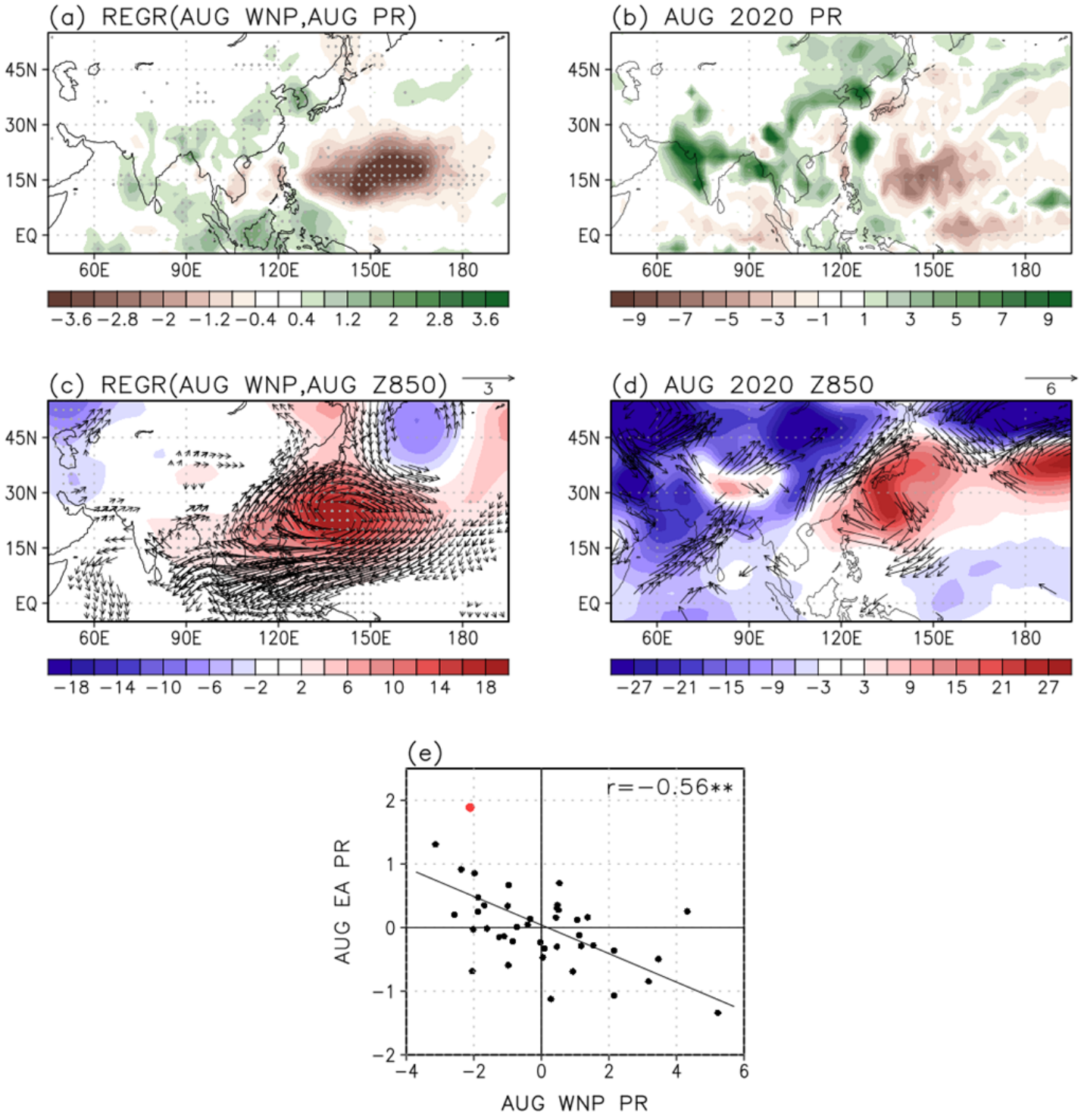

Figure 4

Regressed (a) rainfall (mm/day), (c) geopotential height (shading; m) and wind (vectors; m/s) anomalies at 850 hPa onto the subtropical WNP (140°E-180°, 10°-30°N) rainfall in August during 1979-2020. Note that the regression coefficients are multiplied by the value of subtropical WNP rainfall in August 2020. Values over the 95% confidence level based on the student t-test are stippled and represented as vectors.

(b) Rainfall, (d) geopotential height and wind anomalies at 850 hPa in August 2020. (e) Scatter diagram between the subtropical WNP and East Asian (100°-135°E, 30°-50°N) rainfall index in August. The value for 2020 is indicated by the red dot. The symbol of ** denotes the 99% confidence level based on the student t-test.

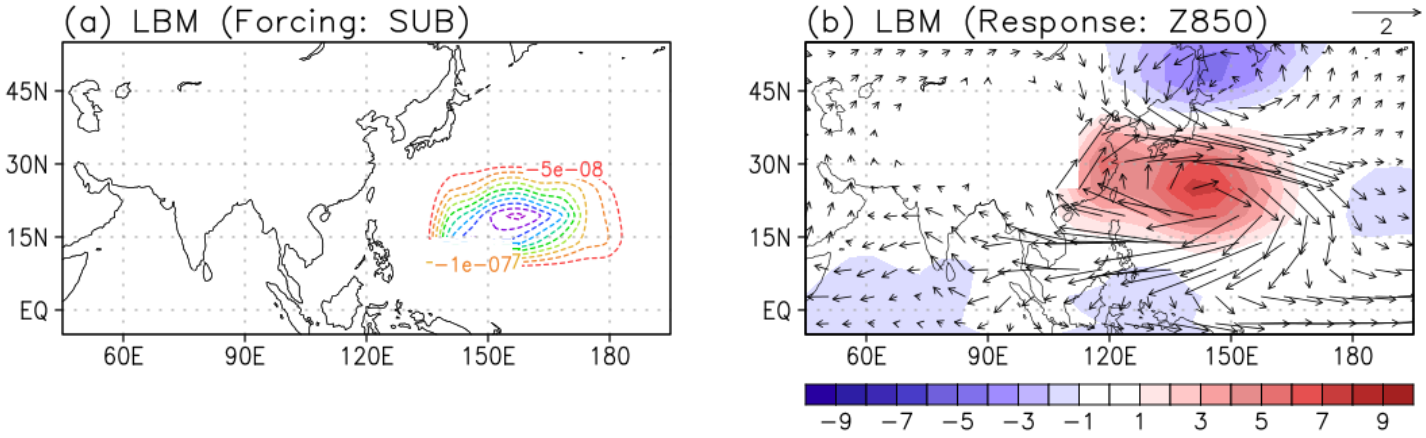

Figure 5

(a) The subtropical WNP (140°E-180°, 10°-30°N) diabatic forcing for LBM simulation based on the regressed rainfall pattern in Fig. 4a. (b) The geopotential height (shading; m) and wind (vector; m/s) anomalies of LBM simulation in August at 850 hPa during 1979-2020 for the forcing in the (a).

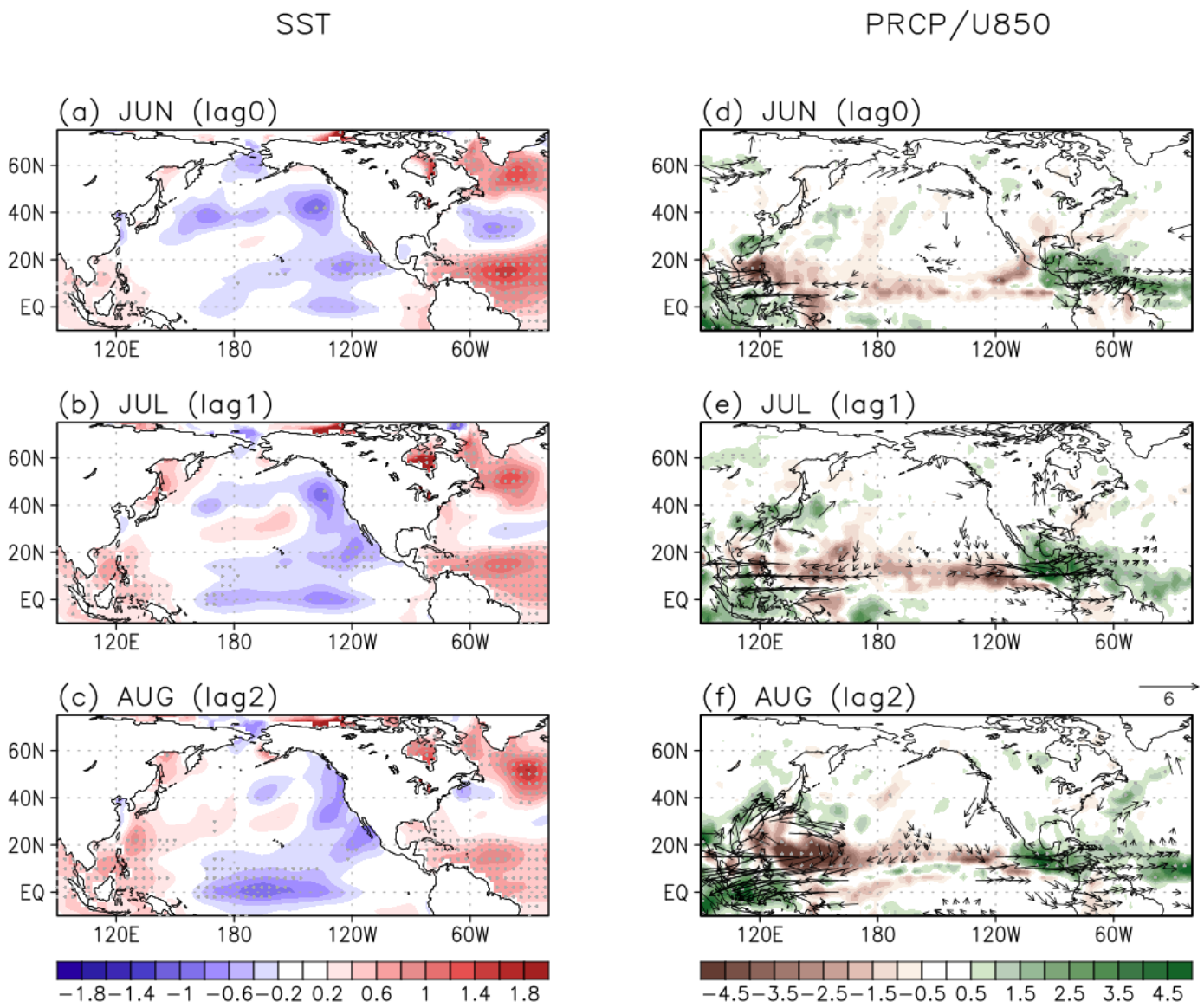

Figure 6

Regressed (left) SST (℃), (right) rainfall (shading; mm/day) and wind (vectors; m/s) anomalies at 850 hPa from June to August onto the NTA (50°-15°W, 0°-20°N) SST in June during 1979-2020, respectively. Values over the 95% confidence level based on the student t-test are stippled and represented as vectors.

Supplementary Files

This is a list of supplementary files associated with this preprint. Click to download.

- SupplementaryInformation.pdf